SANDSTONES AND CONGLOMERATES AT THE FOOTHILLS OF MOUNT SHARP, GALE CRATER, MARS: FACIES ANALYSIS AND STRATIGRAPHIC IMPLICATIONS. K. M. Stack,[1] R. M. E. Williams[2], J. P. Grotzinger[3], D. M. Rubin[4], J. Frydenvang[5], C. H. Seeger[3]. [1]Jet Propulsion Laboratory, California Institute of Technology, 4800 Oak Grove Drive, Pasadena, CA 91104 (kathryn.m.stack@jpl.nasa.gov), [2]Planetary Science Institute, Tucson, AZ, 85719, [3]California Institute of Technology, Pasadena, CA 91125, [4]UC Santa Cruz, Santa Cruz, CA, [5] University of Copenhagen, Denmark.

Introduction: The Mars Science Laboratory (MSL) Curiosity rover's traverse of the foothills of Aeolis Palus (informally Mount Sharp), particularly between Amargosa Valley and Marias Pass (sols 740-970, Fig. 1), offered a prime opportunity to document the stratigraphic relationship and sedimentary facies of the Bradbury group [1], the Mount Sharp group Murray formation [2], and the Siccar Point group Stimson formation [3-5]. This study focuses on a series of sandstone and conglomerate outcrops observed by the Curiosity team in northern Amargosa Valley and along the Lewis and Clark Trail between Pahrump Hills and Marias Pass (Fig. 1) that have been largely overlooked by past studies in the region. Since these key outcrops are located at the contacts between the main units explored by the rover, they have the potential to shed new light on the stratigraphy of Gale crater's sedimentary rock record. Through detailed facies analysis, we seek to understand the depositional origin of these outcrops and their stratigraphic relationship to the major geologic units of Gale crater.

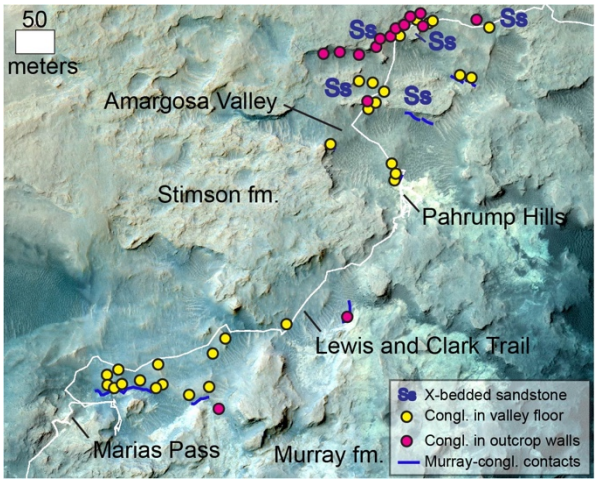

Figure 1. Mapped distribution of conglomerate and sandstone outcrops examined in this study.

Sedimentary Facies: Facies were distinguished on the basis of grain size, sedimentary structures, and bedding style using images from Curiosity's Navigation Cameras (Navcam), Mast Cameras (Mastcam), Chemistry Camera (ChemCam) remote micro-imager (RMI), and the Mars Hand Lens Imager (MAHLI).

Decimeter-scale cross-stratified sandstone. This facies contains a variable abundance of light-toned, well-rounded grains with observable grain diameters averaging ~0.87 mm (coarse sand) and ranging from ~0.4 mm (medium sand) to 1.5 mm (very coarse sand). Mm-thick laminations, some intervals of which exhibit extremely even and regular thickness (Fig. 2b), form low- to moderately-inclined sets exhibiting maximum apparent foreset dip angles of ~25-30º (Fig. 2a). Maximum preserved set thickness reaches ~60 cm, and sets are sometimes bounded and truncated by horizontal to sub-horizontal planar laminae. Foreset dip directions to the northeast and south are most commonly observed. A subfacies characterized by abundant diagenetic nodules, a coarser grain size (coarse sand to pebble size) (Fig. 2d), and moderately to poorly expressed laminations typically comprises the basal portion of exposures of this facies. Cm-scale polygonal fracture patterns exposed along bedding planes and a vertically oriented, light-toned halo around a central fracture (Fig. 2c) are observed to cross-cut laminations of this facies.

Interpretation. Based on the thickness and prevalence of cross-bedded sets, the prevalence of mm-scale uniform laminae, and similarities between these sandstone outcrops and occurrences of Stimson formation sandstone at Marias Pass and Bridger Basin [5], an eolian dune interpretation is favored for this facies.

Conglomerate and pebbly sandstone facies. The conglomerate and pebbly sandstone facies is composed predominantly of moderately rounded clasts in a moderately sorted, clast-supported framework (Fig. 2d). Grains range in size from 0.2 mm (fine sand) to 4.4 mm (fine gravel) and the percent of gravel in conglomerate outcrops ranges from ~15-60%. The matrix is composed predominantly of sand-sized, light-toned grains. Clast imbrication is generally not observed, though there are several instances of possible north-dipping imbrication of tabular clasts (Fig. 2e). This facies is weakly cemented and outcrop exposures are typically discontinuous and poorly preserved resulting in a generally massive appearance with only rare instances of crude stratification and vertical size grading.

Interpretation. The clast-supported texture, moderate sorting, variable rounding, and clast diversity of conglomerate and pebbly sandstones are consistent with transport by water in a fluvial setting either as sheetflood or streamflood flows. The interbedding of conglomerate with pebbly sandstone beds suggests size

sorting resulting from variable sediment transport conditions, and moderate rounding of pebbles is likely due to bedload collision during transport.

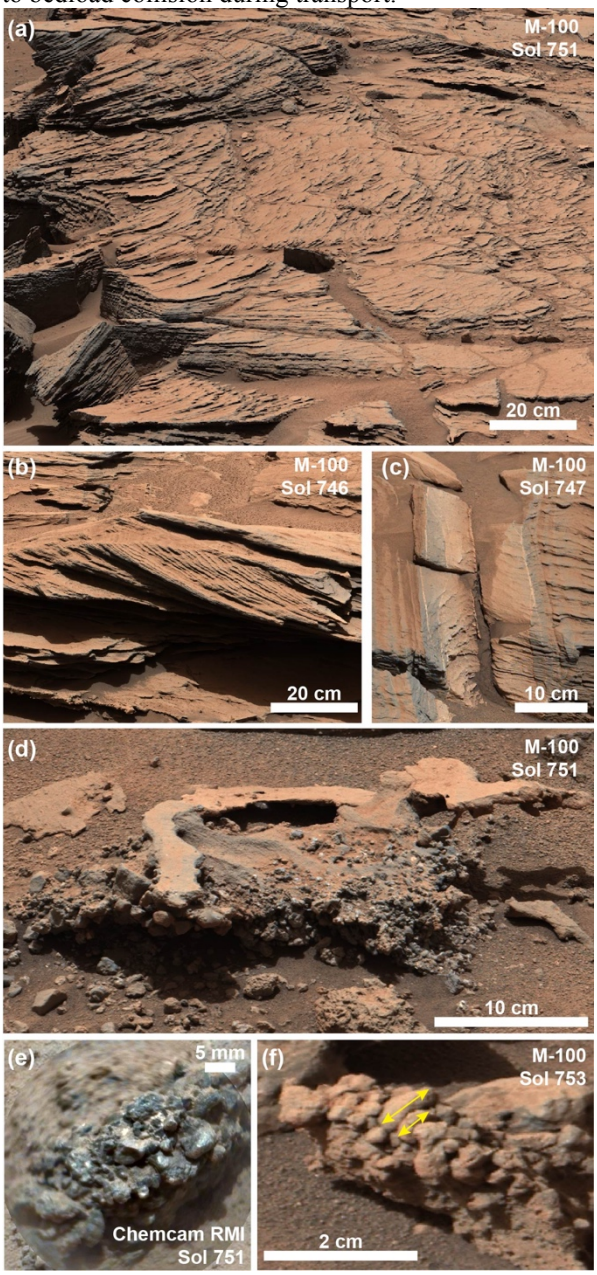

Figure 2. Decimeter-scale cross-bedded sandstone: (a) cross-bedded set at Upheaval Dome, (b) uniform laminations in the north wall of Amargosa Valley, (c) light-toned halo at target Teakettle Junction, (d) coarse pebbles interbedded with sandstone at the base of the cross-bedded sandstone at Upheaval Dome, (e) ChemCam RMI mosaic of Amargosa Valley conglomerate target Shinarump merged with Mastcam M-100, (f) possible northward imbricated clasts in Piute target in Amargosa Valley.

Stratigraphic Context: Exposures of conglomerate and pebbly sandstone were observed in the walls of Amargosa Valley and in low-relief mounds intermittently exposed along the valley floor extending to the base of Marias Pass (Fig.1). The nature of the contact between the conglomerate and pebbly sandstone facies and the Murray formation is ambiguous throughout much of the study area, although occurrences of conglomerate appear to overlie the Murray formation at several locations along the Lewis and Clark Trail. Throughout Amargosa Valley, conglomerate outcrops are observed to grade conformably into overlying pebbly sandstone interbeds at the base of the cross-stratified sandstone outcrops (e.g., Fig. 2d). Decimeter-scale cross-stratified sandstone forms a caprock for the walls and mesas within Amargosa Valley (Fig. 1), but is not observed along the Lewis and Clark Trail.

Discussion. Similarities between the cross-stratified sandstones observed in northern Amargosa Valley and those of the Stimson formation observed at Marias Pass and Bridger Basin are striking, particularly the characteristic set thickness, prevalence of trough cross-beds, and the presence of light-toned halos and distinct rounded white clasts, though these characteristics may not necessarily be unique to the Stimson formation. If the cross-bedded sandstone observed throughout Amargosa Valley is indeed eolian Stimson formation, the conformable relationship between the eolian cross-bedded sandstone and underlying fluvial pebbly sandstone and conglomerate suggests that these outcrops may belong to the Siccar Point group, and thus unconformably overlie the Murray formation.

The occurrence of a Siccar Point group conglomerate along the edge of Aeolis Palus would raise several interesting possibilities. First, it would support fluvial deposition associated with some of the stratigraphically youngest rocks—if the Amargosa sandstones are Stimson fm—thus far encountered by the Curiosity rover. Second, given the textural and geochemical similarities between the conglomerates described here and those found throughout Bradbury Rise [6], it raises the possibility that Siccar Point group conglomerates could be more extensive throughout Aeolis Palus. Thus, some portion of the fluvial stratigraphy observed throughout Bradbury Rise may not be among the oldest rocks in Gale crater as suggested in [5], but rather represent much younger, unconformable deposition at the base of the Gale crater mound, perhaps associated with deposition of the Peace Vallis fan [7], north-to-south flowing deposition originating from Mount Sharp [8], or interfingering from both sources.

References: [1] Grotzinger, J. P. et al. (2014) *Science, 343*. [2] Grotzinger J. P. et al. (2015) *Science, 350,* 6257. [3] Fraeman, A. A. (2016) *JGR Planets, 121(9)* 1713-1736. [4] Watkins, J. et al. (2016) *LPS XLVII,* Abstract #2939, [5] Banham, S. G. et al. (2016) *LPS XLVII* Abstract #2346, [6] Mangold, N. et al. (2016), *JGR Planets, 121*, 353-387, [7] Palucis M. C. et al. (2014), *JGR Planets, 119*, 705-728, [8] Williams, R. M. E. et al. (2018), *Icarus*.